Bioorganic & Medicinal Chemistry 17 (2009) 2030–2037

Contents lists available at ScienceDirect

Bioorganic & Medicinal Chemistry

journal homepage: www.elsevier.com/locate/bmc

BRACO19 analog dimers with improved inhibition of telomerase and hPot 1

Yuan-Te Fu, Brian R. Keppler, Joana Soares, Michael B. Jarstfer *

Division of Medicinal Chemistry and Natural Products, Eshelman School of Pharmacy, The University of North Carolina at Chapel Hill, Chapel Hill, NC 27599-7360, USA

ARTICLE INFO

Article history:
Received 12 September 2008
Revised 8 January 2009
Accepted 9 January 2009
Available online 15 January 2009

Keywords:
Telomerase
hPot1
G-Quadruplex
Acridines
Telomere

ABSTRACT

Human chromosomes terminate with telomeres, which contain double-stranded G-rich, repetitive DNA followed by a single-stranded overhang of the G-rich sequence. Single-stranded oligonucleotides containing G-rich telomeric repeats have been observed in vitro to fold into a variety of G-quadruplex topologies depending on the solution conditions. G-quadruplex structures are notable in part because G-quadruplex ligands inhibit both the enzyme telomerase and other telomere-binding proteins. Because telomerase is required for growth by the majority of cancers, G-quadruplex-stabilizing ligands have become an attractive platform for anticancer drug discovery. Here, we present the preparation and biochemical activities of a novel series of 3,6-disubstituted acridine dimers modeled after the known G-quadruplex ligand BRACO19. These BRACO19 Analog Dimer (BAD) ligands were shown to bind to human telomeric DNA and promote the formation of intramolecular G-quadruplexes in the absence of monovalent cations. As expected, the BAD ligands bound to telomeric DNA with a 1:1 stoichiometry, whereas the parent compound BRACO19, a monomer, bound with a 2:1 stoichiometry. The BAD ligands exhibited potent inhibition of human telomerase with IC_{50} values similar to or lower than those of BRACO19. Furthermore, the BAD ligands displayed greater potency in the inhibition of hPot1 and increased selectivity for G-quadruplex DNA when compared to BRACO19. Collectively, these experiments support the hypothesis that there is an increased potency and selectivity to be gained in the design of G-quadruplex-stabilizing agents that incorporate multiple interactions.

1. Introduction

Telomeres are the DNA–protein complexes that define the ends of eukaryotic chromosomes and function as a cap to protect chromosome ends from unwanted cellular activities such as DNA recombination and degradation.[1,2] Human telomeric DNA is typically comprised of 5–12 kb of a repetitive, double-stranded DNA (5′-TTAGGG-3′/3′-AATCCC-5′) followed by a 150- to 300-nucleotide, guanosine-rich, single-stranded 3′-overhang.[3] In normal somatic cells, telomeric DNA shortens by approximately 50–200 bases during each cell cycle due to inefficient replication of linear chromosomes by the normal DNA replication machinery and apparent degradation.[4] This routine loss of telomeric DNA, which eventually results in chromosomal instability, is offset in the majority of cancer cells by the action of telomerase.[5] Telomerase is a ribonucleoprotein with reverse transcriptase activity that specifically extends the G-rich strand of telomeric DNA,[5] and telomerase activity is routinely observed in the majority of tumor cells, but is not detected in normal somatic cells.[6] As a result, cancer cells increase their replicative lifespan indefinitely by extending and maintaining the length of their telomeres.[1] Because telomere maintenance is required for continuous cellular proliferation, and because telomerase is differentially expressed in cancer cells when compared to normal cells, selective telomerase inhibitors have been sought as an anticancer drug approach.[7]

Single-stranded, G-rich telomeric DNA is capable of folding into four-stranded intramolecular quadruplex structures containing a tetrad of G–G base pairs.[8] Several conformations of G-quadruplexes formed by the human telomeric DNA sequence have been observed (Fig. 1). An antiparallel G-quadruplex topology has been determined by a combined NMR and molecular dynamics approach for the solution structure of a human telomeric sequence in the presence of Na^+.[9] The crystal structure of a K^+-stabilized quadruplex formed by human telomeric DNA was found to be in a parallel propeller-like arrangement.[10] However, the solution structure of a K^+-stabilized human telomeric DNA was reported independently by two separate groups to exhibit a mixed type structure with three of the strands parallel to each other and one strand antiparallel.[11–14]

It is necessary for the RNA template of telomerase to associate with the G-rich single strand of the telomere to effectively catalyze DNA repeat addition. Several reports have demonstrated that telomerase from several species cannot utilize intramolecular G-quadruplex structures as a primer for DNA synthesis,[15–17] and telomerase activity is perturbed by G-quadruplex formation.[18] Based on the seminal observation by Zahler et al.,[15] several groups have explored G-quadruplex-binding ligands as a small-molecule

* Corresponding author. Tel.: +1 919 966 6422; fax: +1 919 966 0204.
E-mail address: jarstfer@unc.edu (M.B. Jarstfer).

0968-0896/$ - see front matter © 2009 Elsevier Ltd. All rights reserved.
doi:10.1016/j.bmc.2009.01.015

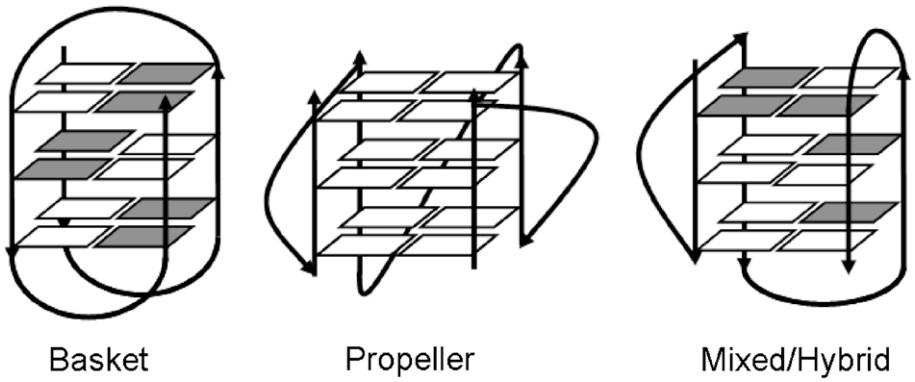

Figure 1. Folding topologies of G-quadruplexes of the human telomeric DNA sequence. Basket-type structures contain alternating parallel/antiparallel G-strands, propeller-type structures contain all parallel G-strands, and hybrid-type structures contain three parallel and one antiparallel G-strands.

approach towards telomerase inhibition.[19] Accordingly, a number of polycyclic chromophores have been shown to inhibit telomerase activity by inducing or stabilizing G-quadruplexes (Fig. 2).[20–23] One of the more promising G-quadruplex-binding compounds, BRACO19, was identified from a series of acridine derivatives with appropriate aminoalkylamido side chains that were reported to stabilize G-quadruplexes with enhanced selectivity for G-quadruplexes compared to duplex DNA.[24–26]

In addition to the requirement of telomerase to synthesize and maintain telomeric DNA, several telomere-binding proteins are necessary to establish proper telomere functions.[27] One such protein, human Protection of telomeres 1 (hPot1), can bind to single-stranded telomeric DNA and is involved in the regulation of telomere length in human cells.[28–32] The crystal structure of the DNA-binding domain of hPot1 reveals that one of the two oligonucleotide/oligosaccharide-binding folds binds and protects the 3′-end of the telomeric single-stranded DNA.[33] Inhibition of hPot1, either by expressing a dominant negative form or by siRNA knockdown leads to a DNA damage response and telomere dysfunction.[30,34] Not surprisingly, the G-quadruplex-binding ligand telomestatin has been shown to disrupt the interaction of both hPot1 and a second telomere-binding protein TRF2 with the telomere.[35–37]

Several other potential G-quadruplexes exist within human chromosomes, and interestingly these appear to be enriched in promoter regions.[38,39] Thus, G-quadruplex-binding ligands have the potential to affect human biology by several mechanisms. One of the greatest challenges in this field is the production of ligands with significant selectivity for specific G-quadruplex DNA structures as compared to canonical dsDNA. In our initial efforts to investigate strategies towards enhanced G-quadruplex specificity, we considered that multiple interactions between the quartet of the G-quadruplex and the binding ligands would be effective. To study this hypothesis, we synthesized a small series of 3,6-disubstituted acridine dimers, which we term BAD compounds (BRACO19 Analog Dimer) and studied their ability to interact with single-stranded telomeric DNA, a model that mimics the 3′ telomeric overhang. Assays were conducted to examine the perturbation of the binding of hPot1 protein to telomeric sequences and the inhibition of telomerase activity in the presence of these G-quadruplex ligands. The results of these studies are reported here.

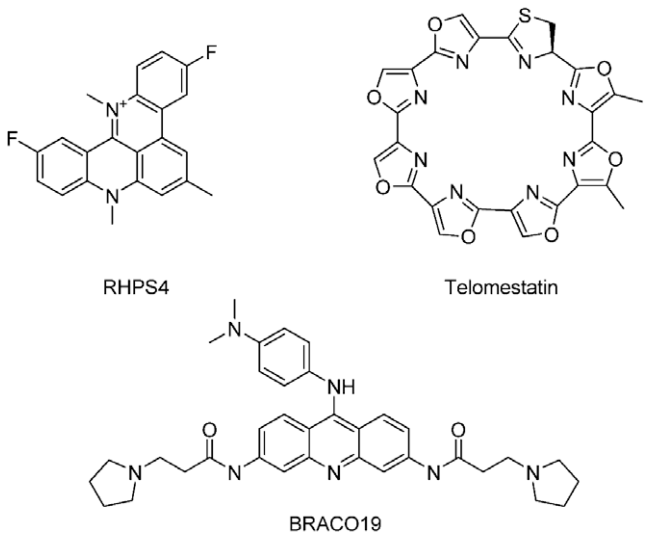

Figure 2. Examples of potent G-quadruplex-binding agents.

2. Results

Taking advantage of the known ability of BRACO19 to interact with G-quadruplex DNA, we synthesized 3,6-disubstituted diacridines dimers connected through the C-9 position of the acridine moiety by a series of linkers (Scheme 1). We anticipated that such compounds would enjoy an enhanced G-quadruplex affinity and specificity compared to the monomeric compounds by virtue of the increased number of complementary interactions between the dimers and the G-quartets within the G-quadruplexes.

2.1. Synthesis of G-quadruplex-binding ligands

Three BRACO19 analog dimers, which we called BAD1, BAD2, and BAD3, were prepared by the simple substitution reaction of the known 9-chloroacridine with the corresponding diamines (Scheme 1). These diamines were chosen in order to match the distance between aromatic rings with the terminal quartets of the G-quadruplex structure. After several failed attempts using mild conditions including refluxing the diamines in the presence of the chloroacridine in chloroform, we found that moderate heat in the presence of phenol was required to permit transformation. The free bases of the diacridines were only sparingly soluble in water and were therefore converted into hydrochloride salts to improve their solubility in aqueous solutions.

2.2. Binding of G-quadruplex ligands to telomeric DNA revealed by circular dichroism

The interactions of BRACO19, BAD1, BAD2, and BAD3 with 3.5 repeats of human telomeric DNA were monitored using CD spec-

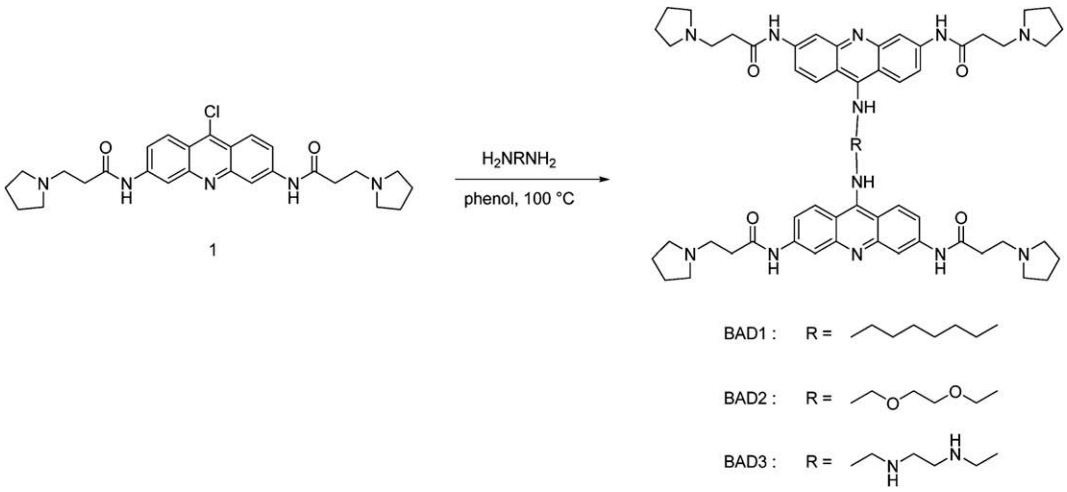

Scheme 1. Synthesis of BAD1, BAD2, and BAD3.

troscopy. In the absence of K^+, Na^+, or G-quadruplex-binding ligand, the CD spectrum of the human telomeric oligonucleotide d[5′-$G_3(T_2AG_3)_3$-3′] was found to show a major positive band at 250 nm, and a minor band at 295 nm (Fig. 3a and b). Upon addition of 2 mol equiv of BRACO19 the CD spectrum showed a dramatic change, as the new spectrum revealed a major positive band at 292 nm and a major negative band at 260 nm (Fig. 3a). This suggested the ligand-induced formation of a G-quadruplex structure. Upon addition of only 1 mol equiv of BAD2 to d[5′-$G_3(T_2AG_3)_3$-3′], the CD spectrum showed a major positive band at 290 nm and a major negative band at 265 nm (Fig. 3b). Similar results were observed for BAD1 and BAD3 (data not shown). The patterns of these CD spectra are characteristic of intramolecular basket G-quadruplex structures, though hybrid, mixed type structures cannot be ruled out.[22]

The ability of the BAD series of compounds to stabilize G-quadruplex DNA was compared to BRACO19 by observing the temperature dependent changes in the UV absorbance at 290 nm. We found that the dimers offered a modest enhancement of G-quadruplex stabilization when compared to BRACO19 (Table 1).

To determine the stoichiometry of the binding of BRACO19 and BAD1–3 to human telomeric G-quadruplexes, titrations of these ligands into a fixed concentration of human telomeric DNA were carried out (Fig. 3). A 15-μM solution of d[5′-$G_3(T_2AG_3)_3$-3′] was incrementally titrated with 0.5 mol equiv of BRACO19. After each addition of BRACO19, samples were allowed to equilibrate for at least 15 min or until no elliptic changes were observed, and CD spectra were recorded. The positive band around 292 nm significantly increased until a 2:1 ratio of BRACO19 to d[5′-$G_3(T_2AG_3)_3$-3′] was reached (Fig. 3c). The titration of a 15-μM solution of d[5′-$G_3(T_2AG_3)_3$-3′] with BAD2 also showed an increase of the positive band around 292 nm. More importantly, the positive 292 nm band significantly increased until a 1:1 ratio of BAD2 to DNA was obtained and further addition of compound had no affect (Fig. 3b and d). Similarly, the titration of BAD1 and BAD3 exhibited an increase in the 292 nm band until a 1:1 ratio of ligands to DNA was reached (data not shown). Of note, in each case further increasing the amount of ligand generally resulted in the precipitation of the DNA, presumably from the formation of insoluble aggregates of the DNA–ligand complexes.

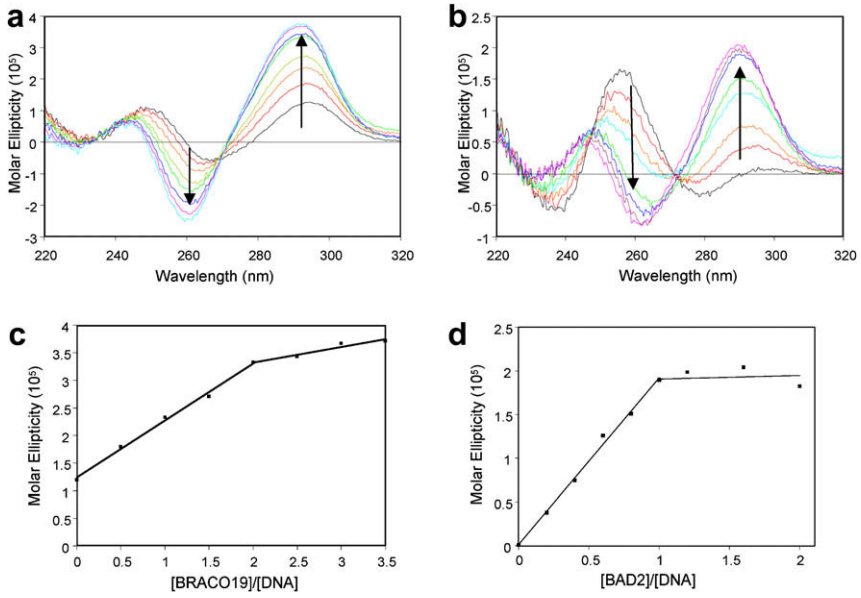

Figure 3. CD spectra of titration of d[5′-$G_3(T_2AG_3)_3$-3′] with (a) BRACO19 and (b) BAD2. Molar ellipticity monitored at 292 nm versus ligand/DNA ratio in the titration of (c) BRACO19 and (d) BAD2.

Table 1
BAD1-3 affect on the thermal stabilization of G-quadruplex DNA and inhibit telomere-binding proteins

Compound	$\Delta T_{1/2}$[a]	Telomerase IC_{50}[b]	hPot1 IC_{50}
BRACO19	18	5.4 (380 nM)	63
BAD1	23	4	17
BAD2	20	9	45
BAD3	28	7.5 (230 nM)	11

[a] Change in melting temperature of d[5′-$G_3(T_2AG_3)_3$-3′] (5 μM) in the presence of 25 μM compound.
[b] Concentration required to achieve 50% inhibition of telomerase in a direct telomerase assay. Values in parenthesis are from experiments with immunopurified telomerase.

2.3. Inhibition of telomerase by G-quadruplex binding ligands

G-Quadruplex-binding ligands are known to inhibit telomerase activity.[40] Initially, we used the PCR-based TRAP assay to examine telomerase inhibition but found that G-quadruplex ligands inhibit the PCR amplification of telomeric DNA, precluding the simple use of this assay for these types of inhibitors. To test the ability of BAD1–3 to inhibit telomerase, we instead examined the concentration dependence of their inhibition by a direct telomerase assay. Recombinant human telomerase was preassembled in vitro and assayed, as a crude preparation, in the absence or presence of varying concentrations of BRACO19 or BAD1–3. These compounds were shown to be effective inhibitors of human telomerase activity, exhibiting IC_{50} values for BAD1–3 (4.0, 9.0, and 7.5 μM, respectively) that were similar to that of BRACO19 (5.4 μM) (Fig. 4). These assays were conducted using unpurified human telomerase in rabbit reticulocyte lysates, which were used to reconstitute the holoenzyme. Upon using immunopurified recombinant telomerase, we found that BRACO19 and BAD3 were apparently more potent in the absence of rabbit reticulocyte lysate with IC_{50} values of 380 nM (lit.[25] = 115 nM) and 230 nM, respectively. The lower observed inhibition in the crude preparation has been previously observed and is likely attributed to the high levels of albumin and other proteins in the reticulocyte lysate that interact with the inhibitors.[41]

2.4. Inhibition of hPot1 binding to telomeric DNA by G-quadruplex binding ligands

In addition to inhibiting telomerase, G-quadruplex ligands can be expected to inhibit other telomere-binding proteins. One protein proven to be affected by G-quadruplex stabilizers is the human single-stranded telomere DNA binding protein hPot1.[16,35] The effects of BRACO19 and BAD1–3 on the binding of human hPot1 protein to single-stranded human telomeric DNA were therefore studied using an affinity separation assay. Recombinant, full-length, ^{35}S-labeled hPot1 was incubated with biotin-labeled human telomeric DNA in the absence or presence of varying concentrations of BRACO19 or BAD1–3 and the resulting hPot1–DNA complexes were captured on streptavidin beads and quantified (Fig. 5). BRACO19 effectively inhibited the binding of hPot1 to telomeric DNA, and the diacridines were found to be even more potent. The IC_{50} values for BRACO19 and BAD1–3 inhibition of hPot1 binding were found to be 63, 17, 45, and 11 μM, respectively. BAD3 appeared to be the most potent compound of the ligands examined.

2.5. Specificity of G-quadruplex-binding ligands revealed by polymerase stop assay

One of the main issues in targeting G-quadruplex DNA is the ability to selectively bind G-quadruplexes in the presence of an overwhelming excess of duplex DNA found in the nucleus. To evaluate the specificity of the interaction between BRACO19 or BAD1–3 with DNA, we employed a DNA polymerase stop assay.[42] Taq DNA polymerase primer extension reactions were carried out using two separate DNA templates. One contained four repeats of the human telomeric sequence, Temp$[TTAGGG]_4$ and a second contained four repeats of a non-G-quadruplex-forming sequence, Temp$[TTAGAG]_4$. Primer extension reactions were conducted in the absence or presence of varying concentrations of BRACO19 and BAD1-3. Using Temp$[TTAGGG]_4$, ligand-induced polymerase stop products at the G-quadruplex-forming site increased upon increasing the concentrations of ligands (Fig. 6). However, higher concentration of ligands increased nonspecific inhibition of the ligands as indicated by the observed accumulation of products at the primer site. The EC_{50} values for BRACO19 and BAD1–3 to inhibit the DNA synthesis of Temp$[TTAGGG]_4$ by Taq polymerase were found to be 1.8, 0.85, 0.20, and 0.071 μM, respectively. The primer extension reactions using the non-G-quadruplex-forming Temp$[TTAGAG]_4$ instead revealed no G-quadruplex stop products (Fig. 7). This indicates that the inhibition of polymerase activity when using this template is due to non-specific interactions of the ligands with the DNA or the enzyme. The EC_{50} values for BRACO19 and BAD1–3 to inhibit the DNA synthesis of Taq polymerase using Temp$[TTAGAG]_4$ were found to be 19.1, 4.5, 3.9, 0.36 μM, respectively. Each of the compounds was therefore 5- to 20-fold more selective for inhibition when the G-quadruplex-forming template was employed. The most selective compound, BAD2, displayed ~20 fold selectivity for increasing stops at the G-quadruplex-forming site, a modest improvement over the ~10-fold selectivity demonstrated by BRACO19.

3. Discussion

Here, we show that 3,6-disubstituted diacridines BAD1–3 are able to induce formation of intramolecular G-quadruplex structures from the human telomeric sequence in the absence of monovalent cations. The interaction of the ligands with the human telomeric G-quadruplex correlates with inhibition of proteins that associate with the telomere including telomerase and hPot1. Our CD studies indicate that the G-quadruplex conformations stabilized by BRACO19 and diacridines BADs1–3 in solution appear to be intramolecular antiparallel G-quadruplexes, though the data do not rule out the possibility of mixed-hybrid types of structures. This contrasts the observation that BRACO19 interacts with the parallel form of the human G-quadruplex in the crystal structures.[43] Importantly, the dimers interacted with G-quadruplex DNA in the expected 1:1 molar ratio indicating that both intercalating moieties enjoyed a binding interaction with the planar surfaces of the G-tetrads. Furthermore, the molar ellipticity of the major positive band around 292 nm significantly decreased upon addition of excess of each ligand, indicating that precipitation of DNA in the solution results at high ligand concentrations. Thus, we infer that the mechanism of telomerase and hPot1 inhibition is related to the ability of BAD dimers to interact directly with DNA and stabilize G-quadruplex structures.

As we were conducting our studies, the G-quadruplex binding agents telomestatin and BRACO19 were reported to inhibit hPot1, which is consistent with our findings.[35,37,44] Given the dramatic effect hPot1 inhibition can have on proliferative cells, which includes the induction of apoptosis in p53-negative cells and induction of senescence in p53-negative cells,[30,34] it is likely that hPot1 inhibition is responsible for the acute cytotoxicity observed with telomere-binding agents. However, the low toxicity of BRACO19 reported in studies using mice bearing human cancer xenografts, suggests that hPot1 inhibition does not cause irreversible damage to normal cells, at least at the doses used in those studies.[45]

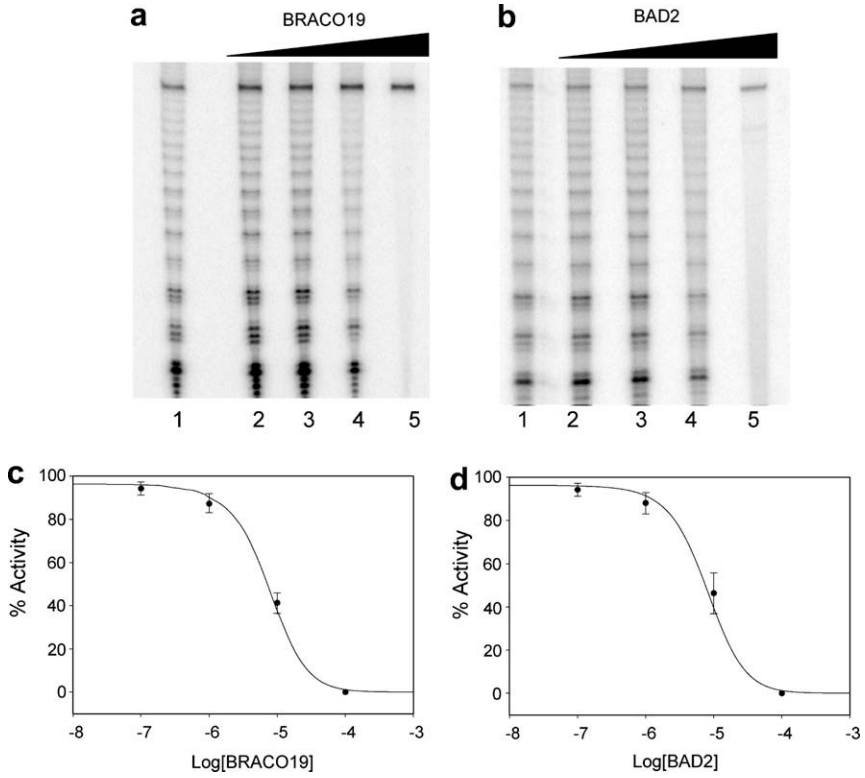

Figure 4. Concentration dependence of telomerase inhibition. (a) Inhibition by BRACO19. Lane 1 contained no inhibitor. The concentrations of BRACO19 in lanes 2–5 were 0.1, 1, 10, and 100 μM, respectively. (b) Inhibition by BAD2. Lane 1 contained no inhibitor. The concentrations of BAD2 in lanes 2–5 were 0.1, 1, 10, and 100 μM, respectively. (c) Dose response curve for telomerase inhibition by BRACO19. (d) Dose–response curve for telomerase inhibition by BAD2.

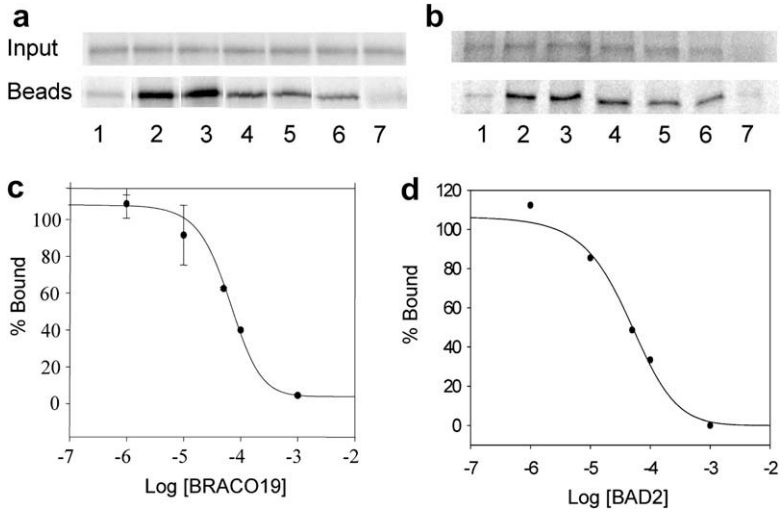

Figure 5. G-quadruplex-binding compounds inhibit hPot1 binding to telomeric DNA. (a) Inhibition of hPot1 binding to telomeric DNA by BRACO19. Lane 1 contained no DNA. The concentrations of BRACO19 for lanes 2–7 were 0, 1, 10, 50, 100, and 1000 μM, respectively (b) Inhibition of hPot1 binding to telomeric DNA by BAD2. Lane 1 contained no DNA. The concentrations of BAD2 for lanes 2-7 were 0, 1, 10, 50, 100, and 1000 μM, respectively. (c) Dose–response curve for hPot1 inhibition by BRACO19. (d) Dose–response curve for hPot1 inhibition by BAD2.

In addition to determining whether G-quadruplex-binding ligands inhibit hPot1, one of the goals of this work was to determine if dimers of BRACO19 would enjoy increased selectivity for G-quadruplex DNA when compared to duplex DNA. The selectivity of the BAD ligands to G-quadruplex DNA versus conical double-stranded DNA was tested using a polymerase stop assay. We found that BAD2 was apparently more selective for G-quadruplex DNA than dsDNA when compared to BRACO19. In addition, it is well established that the dimethylaminoanilino ring on BRACO19 is a critical feature of its potency. In the BAD series of compounds, this ring is removed but the compounds still enjoy greater comparative activity. One promising finding was that the BAD compounds had varying inhibition profiles suggesting that G-quadruplex binding was sensitive to the linker bridging the two chromophores. Thus, we predict that future research aimed at properly designing linkers can be employed to enhance ligand binding affinity and selectivity towards G-quadruplex DNA.

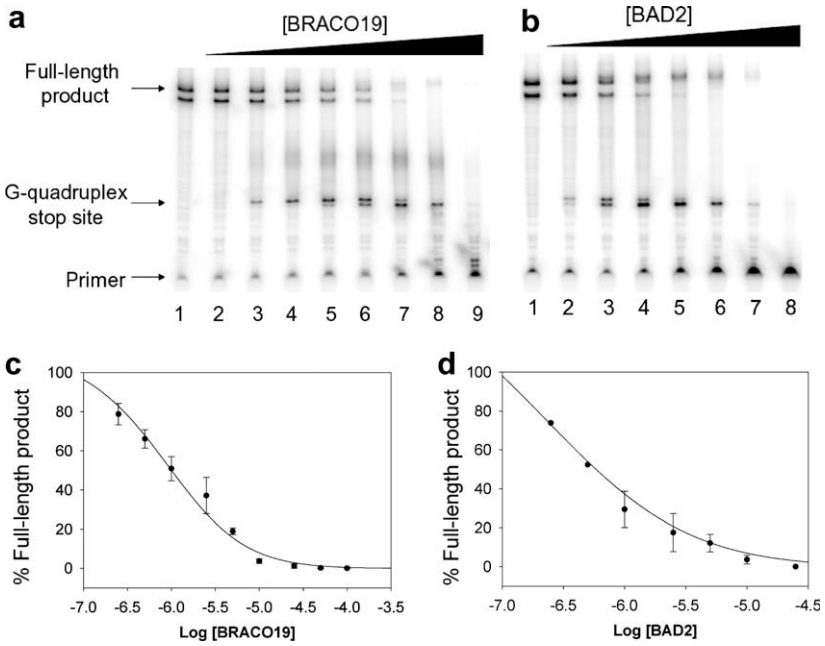

Figure 6. Concentration-dependent blocks of polymerase DNA synthesis by BRACO19 and BAD2 on a DNA template containing the human telomeric sequence $(TTAGGG)_4$. (a) The concentrations of BRACO19 in lanes 1–9 were 0, 0, 0.25, 0.5, 1, 2.5, 5, 10, and 25 μM. (b) The concentrations of BAD2 in lanes 1–8 were 0, 0.25, 0.5, 1, 2.5, 5, 10, and 25 μM. (c) Dose–response curve for polymerase inhibition by BRACO19. (d) Dose–response curve for polymerase inhibition by BAD2.

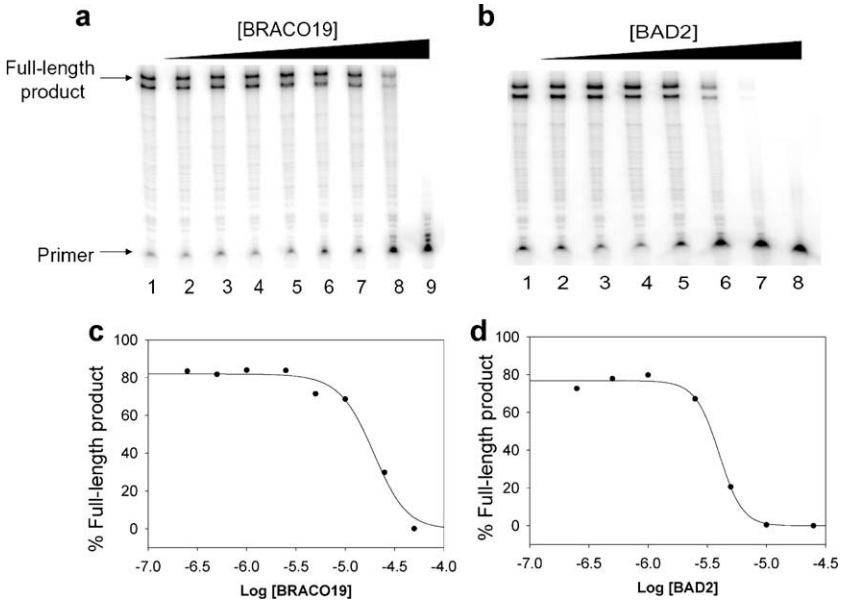

Figure 7. Concentration-dependent blocks of polymerase DNA synthesis by BRACO19 and BAD2 on a DNA template containing a non-telomeric sequence $(TTAGAG)_4$. (a) The concentrations of BRACO19 in lanes 1–9 were 0, 0, 0.25, 0.5, 1, 2.5, 5, 10, and 25 μM. (b) The concentrations of BAD2 in lanes 1–8 were 0, 0.25, 0.5, 1, 2.5, 5, 10, and 25 μM. (c) Dose–response curve for polymerase inhibition by BRACO19. (d) Dose–response curve for polymerase inhibition by BAD2.

4. Materials and methods

4.1. General

^{1}H NMR spectra were recorded on a 300-MHz Varian Gemini 2000 spectrometer. CD spectra were recorded on a Π-star 180 spectrophotometer. Primer 5′-TAATACGACTCACTATAG-3′, DNA templates Temp$[TTAGGG]_4$ 5′-TCCAACTATGTATAC$[TTAGGG]_4$ TTA GCCACGCAATTGCTATA-GTGAGTCGTATTA-3′ and Temp$[TTAGAG]_4$ 5′-TCCAACTATGTATAC$[TTAGAG]_4$TTAGCCACGCAATTGCTA TAGTGA GTCGTATTA-3′, and all other DNAs were purchased from IDT. The synthetic routes for the synthesis of compound 1 and BRACO19 were based on a published method.[25]

4.2. Synthesis of BAD1

A solution of 3,6-bis(3-pyrrolidin-1-ylpropionamido)-9-chloro-acridine[46] (0.10 g, 0.2 mmol) and 1,8-diaminooctane (0.014 g, 0.1 mmol) in 2 mL of phenol was heated at 100 °C for 2 h. The reaction mixture was added to 30 mL of EtOAc. The precipitates were collected by filtration and washed with EtOAc. Precipitates were recrystallized from CH_3OH and EtOAc yielding a yellow solid

(0.057 g, 51%). The free base was obtained by dissolving the solid in CH_3OH and added to a cold 0.1 M NaOH solution. The precipitate was collected, washed with cooled H_2O followed by ethyl ether, and recrystallized from CH_3OH and Et_2O. The hydrochloride salt was prepared by adding a solution of the free base in CH_3OH into saturated ethereal HCl solution, the precipitated solids were collected and washed with EtOAc and Et_2O. ^1H NMR (DMSO-d_6): δ 10.91 (s, 4H), 8.43 (d, 4H), 8.35 (s, 4H), 7.42 (d, 4H), 3.91 (t, 4H), 2.80 (t, 8H), 2.66 (t, 8H), 2.56 (m, 16H), 1.72 (m, 16H), 1.30 (m, 12H). MS (ESI): 1060 (MH+).

4.3. Synthesis of BAD2

Following the procedure for BAD1, compound **1** (0.10 g, 0.2 mmol) was treated with 2,2′-(ethylenedioxy)bis(ethylamine) (0.015 g, 0.1 mmol) to give a yellow solid (0.051 g, 45%). ^1H NMR (DMSO-d_6): δ 10.67 (s, 4H), 8.46 (s, 4H), 8.24 (d, 4H), 7.67 (d, 4H), 3.59 (s, 4H), 3.39 (t, 4H), 3.01 (t, 4H), 2.74 (t, 8H), 2.69 (m, 16H), 2.57 (t, 8H), 1.66 (m, 16H). MS (ESI): 1064 (MH+).

4.4. Synthesis of BAD3

Following the procedure for BAD1, compound **1** (0.10 g, 0.2 mmol) was treated with triethylenetetramine dihydrochloride (0.022 g, 0.1 mmol) to give a yellow solid (0.046 g, 41%). ^1H NMR (DMSO-d_6): δ 10.32 (s, 4H), 8.13 (d, 4H), 8.08 (s, 4H), 7.27 (s, 4H), 2.81 to 2.55 (m, 20H), 2.45 (m, 24H), 1.63 (m, 16H). MS (ESI): 1062 (MH+).

4.5. CD Spectroscopy

CD spectra were recorded on a Π-star 180 spectropolarimeter using a quartz cell of 1-mm optical path length and scanned at 25 °C with a speed of 100 nm/min with a response time of 1 s. DNA samples were dissolved in TE (10 mM Tris–HCl, pH 7.5, and 1 mM EDTA) resulting in a concentration of 15 μM. DNA samples were prepared by heating at 95 °C for 5 min and cooling to room temperature. Hydrochloride salts of BRACO19 and BAD1–3 were dissolved in H_2O and titrated into the DNA samples. After each addition of ligands, the reactions were allowed to equilibrate for at least 15 min to collect the CD spectra.

4.6. Reconstitution and immunopurification of telomerase

Wild-type hTR was in vitro transcribed and purified as previously described except that the Ampliscribe T7 Transcription Kit was used (Epicentre Technologies).[47] Flag-tagged hTERT was transcribed and translated from pCR3.1-Flag–hTERT using the TNT Coupled Rabbit Reticulocyte Lysate Systems Kit (Promega). The expression construct for Flag–hTERT was a gift from Dr. Lea Harrington (University of Toronto). A 400 μL reaction contained 8 μg of pCR3.1-Flag-hTERT, 16 μL of [^{35}S]-methionine (1175 Ci/mmol, 10 μCi/μl; Perkin-Elmer), 4 μg of in vitro transcribed hTR, and other components provided in the kit as described by the manufacturer. Flag-tagged hTERT was immunoprecipitated with anti-FLAG M2 affinity agarose beads (Sigma–Aldrich, St. Louis, MO). Beads (50 μL) were washed four times in 400 μL of IP buffer (10 mM Tris–Cl, pH 7.5, 100 mM KCl, 1 mM $MgCl_2$, 10% glycerol, 0.1 mM DTT), and centrifuged at 1500*g* for 2 min between washes. Reticulocyte lysate translation reaction (45 μL) was added to 450 μL of 1× Tris IP buffer and centrifuged at 16,000*g* for 15 min at 4 °C to remove any particulates. The supernatant was added to beads and allowed to nutate at 4 °C for 2 h. The beads were washed six times in 400 μL IP buffer centrifuging at 1500*g* for 2 min between washes and resuspended in 20 μL IP buffer. Fractions from the input and washes were kept for further analysis. BSA (3 μL of 10 mg/ml) was added to the beads to prevent protein from sticking to the tube and the bead slurry (~50 μL) was transferred to a Protein LoBind tube (Eppendorf) and washed once in 500 μL TMG (10 mM Tris acetate, pH 8, 1 mM $MgCl_2$, 10% glycerol) centrifuging at 1500*g* for 2 min. Fifty microliters of peptide solution [41 μL TMG, 9 μL FLAG peptide (Sigma, 5 mg/ml in 20 mM Tris acetate, pH 7.5)] was added to the beads and nutated at 4 °C for 1 h. The beads were centrifuged at 1500*g* for 2 min and the eluant was removed and added to a fresh LoBind tube, flash frozen, and stored at −80 °C until used.

4.7. Direct telomerase assay

Telomerase activity was measured using a modified version of a previously described direct assay. Each 25 μL reaction contained 50 mM Tris–HCl, pH 8.0, 50 mM KCl, 1 mM $MgCl_2$, 5 mM β-mercaptoethanol, 1 mM spermidine, 1 μM human telomere primer (5′-TTAGGGTTAGGGTTAGGG-3′), 0.5 mM dATP, 0.5 mM dTTP, 2.9 μM dGTP, 0.33 μM [α-^{32}P]dGTP (3000 Ci/mmol, 10 μCi/μL; Perkin-Elmer), and 10 μL of preassembled telomerase. Inhibition studies also included varying amounts of BRACO19, BAD1, BAD2, or BAD3. Primer extension was carried out at 30 °C for 90 min. After the addition of a ^{32}P-labeled loading control (114 nucleotide, 5′-end labeled DNA oligonucleotide, 1000 cpm per reaction), the primer extension products were extracted with phenol/chloroform/isoamyl alcohol and ethanol precipitated in the presence of 0.6 M NH_4OAc and 35 ng/μL glycogen. Products were precipitated at −80 °C in 2.5 volumes of absolute ethanol for 30 min followed by centrifugation at 22,000*g* at 4 °C for 25 min and washing with 2 volumes of 70% ethanol. Pellets were re-suspended in a suitable volume of TE, and ethanol precipitation was repeated to ensure the removal of all unincorporated [α-^{32}P]dGTP. The final pellets were dissolved in a formamide-loading buffer containing 40% formamide, 10 mM Tris–HCl, pH 8.0, 10 mM EDTA, 0.05% xylene cyanol, and 0.05% bromophenol blue. The products were heated at 95 °C for 5 min and resolved on a prewarmed, 0.4 mm thick, 20 × 20 cm, 10% polyacrylamide/7 M urea/1× TBE gel. The gel was run at 800 V for 1 h in 1× TBE. After drying the gel and exposing it to a phosphorimager screen (Molecular Dynamics) overnight, it was imagined using a phosphorimager (Molecular Dynamics Storm 860), and quantified with ImageQuant (version 5.2).

4.8. hPot1-binding assay

^{35}S-labeled hPot1 protein was synthesized from pCIneo-Flag-hPot1 (from Christopher Counter, Duke University) in vitro using a T7-coupled TNT system. Each binding reaction contained 50 μL of ^{35}S-labeled hPot1 from a crude reticulocyte lysate reaction and 2.5 μL of 1 μM biotin–hTel DNA. Inhibition studies also included various amounts of BRACO19 and BAD1–3. Reactions were incubated at 30 °C for 90 min before using MPG streptavidin beads to isolate bound protein. Each reaction used 45 μL of MPG streptavidin beads. Before use, the streptavidin beads were washed four times with 400 μL of wash buffer 1 (20 mM Tris-acetate, pH 7.5, 10% glycerol, 1 mM EDTA, 5 mM $MgCl_2$, 100 mM potassium glutamate, 0.1% IGEPAL, and 1 mM DTT) and blocked twice with 250 μL of blocking buffer (20 mM Tris-acetate, pH 7.5, 10% glycerol, 1 mM EDTA, 5 mM $MgCl_2$, 100 mM potassium glutamate, 0.1% IGEPAL, 1 mM DTT, 0.5 mg/mL lysozyme, 0.5 mg/mL BSA, 0.05 mg/mL glycogen, and 0.1 mg/mL yeast RNA) for 15 min at 4 °C. Between each washing and blocking step, the beads were precipitated by centrifugation at 2500*g* for 2 min and the supernatant was removed. A total of 60 μL of blocking buffer was then mixed with the 60 μL DNA/protein sample and centrifuged at 17,000*g* for 10 min at 4 °C to remove any precipitates. This supernatant was then added to the blocked beads, and the samples were mixed on a rotator for

2 h at 4 °C. Following mixing, the beads were washed three times with 350 μL of wash buffer 2 (20 mM Tris-acetate, pH 7.5, 10% glycerol, 1 mM EDTA, 5 mM $MgCl_2$, 300 mM potassium glutamate, 0.1% IGEPAL, and 1 mM DTT) and twice with 350 μL of TMG (10 mM Tris-acetate, pH 8.0, 1 mM $MgCl_2$, and 10% glycerol). The beads were precipitated by centrifugation at 2500*g* for 2 min between each wash and the supernatant was removed. The beads were then re-suspended in 1× SDS gel-loading buffer containing 10 mM DTT. Samples were heated for 5 min at 95 °C and the supernatant was loaded onto a 6–8% SDS–PAGE gel. The gel was run at 180 V for 1 h, dried, and exposed to a phosphorimager screen overnight.

4.9. Polymerase stop assays

The 5′-end-labeled single-strand oligonucleotide was prepared by incubating the oligomer with T4 polynucleotide kinase and [γ-^{32}P]ATP at 37 °C for 1 h. The kinase activity was inactivated by heating at 70 °C for 8 min and the labeled primer was purified on a MicroSpin G-25 column (Amersham Biosciences). Labeled DNA primer (15 nM), and templates (10 nM) were annealed in GoTaq buffer with 0.1 mM dNTP by heating at 95 °C for 5 min and were slowly cooled to room temperature. Ligands were added at various concentrations and incubated at room temperature for 30 min. Taq DNA polymerase (2.5 U) was added and the mixtures were incubated at 55 °C for 20 min. The polymerase extension reactions were stopped by adding 2× stop buffer (10 mM EDTA, 10 mM NaOH, 0.1% xylene cyanole, and 0.1% bromphenol blue in formamide solution). Samples were heated at 95 °C for 5 min and were loaded onto a 10% denaturing polyacrylamide gel. The gel was run at 800 V for 1 h. After drying the gel and exposing it to a phosphorimager screen (Molecular Dynamics) overnight, polymerase activity was imaged using a phosphorimager and quantified with ImageQuant.

4.10. UV melting curves

UV melting curves were monitored at 295 nm using d[5′-$G_3(T_2AG_3)_3$-3′] (5 μM) in a buffer of 10 mM K^+ (pH 7.5) containing either 40 mM KCl or test compound (25 μM). A reference cell containing only buffer was also monitored. The temperature was ramped from 10 to 95 °C at a rate of 1 °C min^{-1}. Samples were annealed prior to analysis. Melting temperatures ($t_{1/2}$) were calculated from the first derivative of the absorbance versus temperature curves.

Acknowledgments

This research was supported by the Elsa Pardee Foundation. We thank Dr. Lea Harrington for the Flag-hTERT construct, Dr. Christopher Counter for the hPot1 construct, and Dr. Tracy Bryan for sharing the protocol for immunopurification of Flag-tagged human telomerase. We thank Dr. Ian K. Moon for his assistance in the preparation of this manuscript.

References and notes

1. Blasco, M. A. *Nat. Rev. Genet.* **2005**, *6*, 611.
2. de Lange, T. *Oncogene* **2002**, *21*, 532.
3. Wright, W. E.; Tesmer, V. M.; Huffman, K. E.; Levene, S. D.; Shay, J. W. *Genes Dev.* **1997**, *11*, 2801.
4. Harley, C. B.; Futcher, A. B.; Greider, C. W. *Nature (London)* **1990**, *345*, 458.
5. Autexier, C.; Lue, N. F. *Annu. Rev. Biochem.* **2006**, *75*, 493.
6. Shay, J. W.; Bacchetti, S. *Eur. J. Cancer* **1997**, *33*, 787.
7. Kelland, L. R. *Eur. J. Cancer* **2005**, *41*, 971.
8. Burge, S.; Parkinson, G. N.; Hazel, P.; Todd, A. K.; Neidle, S. *Nucleic Acids Res.* **2006**, *34*, 5402.
9. Wang, Y.; Patel, D. J. *Structure* **1993**, *1*, 263.
10. Parkinson, G. N.; Lee, M. P.; Neidle, S. *Nature* **2002**, *417*, 876.
11. Luu, K. N.; Phan, A. T.; Kuryavyi, V.; Lacroix, L.; Patel, D. J. *J. Am. Chem. Soc.* **2006**, *128*, 9963.
12. Zhang, N.; Phan, A. T.; Patel, D. J. *J. Am. Chem. Soc.* **2005**, *127*, 17277.
13. Ambrus, A.; Chen, D.; Dai, J.; Bialis, T.; Jones, R. A.; Yang, D. *Nucleic Acids Res.* **2006**, *34*, 2723.
14. Dai, J.; Punchihewa, C.; Ambrus, A.; Chen, D.; Jones, R. A.; Yang, D. *Nucleic Acids Res.* **2007**, *35*, 2440.
15. Zahler, A. M.; Williamson, J. R.; Cech, T. R.; Prescott, D. M. *Nature* **1991**, *350*, 718.
16. Zaug, A. J.; Podell, E. R.; Cech, T. R. *Proc. Natl. Acad. Sci. U.S.A.* **2005**, *102*, 10864.
17. Oganesian, L.; Moon, I. K.; Bryan, T. M.; Jarstfer, M. B. *EMBO J.* **2006**, *25*, 1148.
18. Sun, D.; Lopez-Guajardo, C. C.; Quada, J.; Hurley, L. H.; Von Hoff, D. D. *Biochemistry* **1999**, *38*, 4037.
19. Cuesta, J.; Read, M. A.; Neidle, S. *Mini.-Rev. Med. Chem.* **2003**, *3*, 11.
20. Goncalves, D. P.; Ladame, S.; Balasubramanian, S.; Sanders, J. K. *Org. Biomol. Chem.* **2006**, *4*, 3337.
21. Dixon, I. M.; Lopez, F.; Tejera, A. M.; Esteve, J. P.; Blasco, M. A.; Pratviel, G.; Meunier, B. *J. Am. Chem. Soc.* **2007**, *129*, 1502.
22. Shin-ya, K.; Wierzba, K.; Matsuo, K.; Ohtani, T.; Yamada, Y.; Furihata, K.; Hayakawa, Y.; Seto, H. *J. Am. Chem. Soc.* **2001**, *123*, 1262.
23. Cian, A. D.; Delemos, E.; Mergny, J. L.; Teulade-Fichou, M. P.; Monchaud, D. *J. Am. Chem. Soc.* **2007**, *129*, 1856.
24. Read, M.; Harrison, R. J.; Romagnoli, B.; Tanious, F. A.; Gowan, S. H.; Reszka, A. P.; Wilson, W. D.; Kelland, L. R.; Neidle, S. *Proc. Natl. Acad. Sci. U.S.A.* **2001**, *98*, 4844.
25. Gowan, S. M.; Harrison, J. R.; Patterson, L.; Valenti, M.; Read, M. A.; Neidle, S.; Kelland, L. R. *Mol. Pharmacol.* **2002**, *61*, 1154.
26. Harrison, R. J.; Cuesta, J.; Chessari, G.; Read, M. A.; Basra, S. K.; Reszka, A. P.; Morrell, J.; Gowan, S. M.; Incles, C. M.; Tanious, F. A.; Wilson, W. D.; Kelland, L. R.; Neidle, S. *J. Med. Chem.* **2003**, *46*, 4463.
27. de Lange, T. *Genes Dev.* **2005**, *19*, 2100.
28. Baumann, P.; Cech, T. R. *Science* **2001**, *292*, 1171.
29. Yang, Q.; Zheng, Y. L.; Harris, C. C. *Mol. Cell. Biol.* **2005**, *25*, 1070.
30. Veldman, T.; Etheridge, K. T.; Counter, C. M. *Curr. Biol.* **2004**, *14*, 2264.
31. Loayza, D.; De Lange, T. *Nature* **2003**, *423*, 1013.
32. Lei, M.; Zaug, A. J.; Podell, E. R.; Cech, T. R. *J. Biol. Chem.* **2005**, *280*, 20449.
33. Lei, M.; Podell, E. R.; Cech, T. R. *Nat. Struct. Mol. Biol.* **2004**, *11*, 1223.
34. Hockemeyer, D.; Sfeir, A. J.; Shay, J. W.; Wright, W. E.; de Lange, T. *EMBO J.* **2005**, *24*, 2667.
35. Gomez, D.; O'Donohue, M. F.; Wenner, T.; Douarre, C.; Macadre, J.; Koebel, P.; Giraud-Panis, M. J.; Kaplan, H.; Kolkes, A.; Shin-ya, K.; Riou, J. F. *Cancer Res.* **2006**, *66*, 6908.
36. Tahara, H.; Shin-Ya, K.; Seimiya, H.; Yamada, H.; Tsuruo, T.; Ide, T. *Oncogene* **2006**, *25*, 1955.
37. Gomez, D.; Wenner, T.; Brassart, B.; Douarre, C.; O'Donohue, M. F.; El Khoury, V.; Shin-Ya, K.; Morjani, H.; Trentesaux, C.; Riou, J. F. *J. Biol. Chem.* **2006**, *281*, 38721.
38. Huppert, J. L.; Balasubramanian, S. *Nucleic Acids Res.* **2007**, *35*, 406.
39. Lee, J. Y.; Okumus, B.; Kim, D. S.; Ha, T. *Proc. Natl. Acad. Sci. U.S.A.* **2005**, *102*, 18938.
40. Hurley, L. H.; Wheelhouse, R. T.; Sun, D.; Kerwin, S. M.; Salazar, M.; Fedoroff, O. Y.; Han, F. X.; Han, H.; Izbicka, E.; Von Hoff, D. D. *Pharmacol. Ther.* **2000**, *85*, 151.
41. Barma, D. K.; Elayadi, A.; Falck, J. R.; Corey, D. R. *Bioorg. Med. Chem. Lett.* **2003**, *13*, 1333.
42. Han, H.; Hurley, L. H.; Salazar, M. *Nucleic Acids Res.* **1999**, *27*, 537.
43. Campbell, N. H.; Parkinson, G. N.; Reszka, A. P.; Neidle, S. *J. Am. Chem. Soc.* **2008**, *130*, 6722.
44. Gunaratnam, M.; Greciano, O.; Martins, C.; Reszka, A. P.; Schultes, C. M.; Morjani, H.; Riou, J. F.; Neidle, S. *Biochem. Pharmacol.* **2007**, *74*, 2493.
45. Burger, A. M.; Dai, F.; Schultes, C. M.; Reszka, A. P.; Moore, M. J.; Double, J. A.; Neidle, S. *Cancer Res.* **2005**, *65*, 1489.
46. Moore, M. J.; Schultes, C. M.; Cuesta, J.; Cuenca, F.; Gunaratnam, M.; Tanious, F. A.; Wilson, W. D.; Neidle, S. *J. Med. Chem.* **2006**, *49*, 582.
47. Keppler, B. R.; Jarstfer, M. B. *Biochemistry* **2004**, *43*, 334.